Stress Fibers in the Splenic Sinus Endothelium In Situ: Molecular Structure, Relationship to the Extracellular Matrix, and Contractility

Detlev Drenckhahn and Joachim Wagner

Institute of Anatomy and Cell Biology, University of Marburg, D-3550 Marburg, West Germany

Abstract. In the present study, we investigated structural and functional aspects of stress fibers in a cell type in situ, i.e., the sinus endothelium of the human spleen. In this cell type, stress fibers extend underneath the basal plasma membrane and are arranged parallel to the cellular long axis. Ultrastructurally, the stress fibers were found to be composed of thin actin-like filaments (5–8 nm) and thick myosin-like filaments (10–15 nm × 300 nm). Actin filaments displayed changes in polarity (determined by S-1–myosin subfragment decoration), which may allow a sliding filament mechanism. At their plasmalemmal attachment sites, actin filaments exhibited uniform polarity with the S-1–arrowhead complexes pointing away from the plasma membrane. Fluorescence microscopy showed that the stress fibers have a high affinity for phalloidin and antibodies to actin, myosin, tropomyosin, and α-actinin. Vinculin was confined to the cytoplasmic aspect of the plasmalemmal termination sites of stress fibers, while laminin, fibronectin, and collagens were located at the extracellular aspect of these stress fiber–membrane associations. Western blot analysis revealed polypeptide bands that contained actin, myosin, and α-actinin to be major components of isolated cells. Exposure of permeabilized cells to MgATP results in prominent changes in cellular shape caused by stress fiber contraction. It is concluded that the stress fibers in situ anchored to cell-to-extracellular matrix contacts can create tension that might allow the endothelium to resist the fluid shear forces of blood flow.

STRESS fibers represent the most prominent structural component of the actin filament system of most cell types in tissue culture. Their molecular structure and dynamics in various processes of cell biology are subjects of much recent interest (for review, see references 31, 33, and 50). Previous studies have demonstrated stress fibers to occur also in certain cells in situ such as in flattened fibroblasts located underneath scales of fish (10) or in endothelial cells of the vascular system (14, 28, 65, 67). These observations demanded more detailed studies regarding the degree of molecular relationship between stress fibers in vitro and in situ, including their association with components of the extracellular matrix. Apart from these more general aspects, a major concern of the present study was to obtain more detailed insight into structural and functional aspects of vascular endothelial stress fibers, which obviously play a crucial role in maintaining intimal integrity (24, 26–28, 65, 67).

In search of a source of vascular endothelium suitable for these studies, we found that endothelial cells of the sinus vessels in the human spleen have many advantages in comparison to endothelial cells of other vascular segments (14, 15). These advantages are the uniform rod-shaped morphology and parallel alignment of cells, the existence of well-defined sites of contacts to the extracellular matrix, and importantly, a highly ordered pattern of stress fibers. Previous electron microscope studies on the splenic sinus endothelium (11, 13, 14, 35) have shown that bundles of microfilaments (which are shown here to represent typical stress fibers) are oriented parallel to the cellular long axis. Each end of the stress fibers appears to be attached to the basal (abluminal) plasma membrane at sites where the annular component of the basement membrane abuts the endothelial cells (see Fig. 26). This annular component of the basement membrane is identical to the argyrophilic rings, i.e., the ring fibers that enclose the sinus wall like hoops around the staves of a cask (25). Outside their contact zone with ring fibers, endothelial cells lack a basal lamina (11, 13, 35). Thus, sinus endothelial cells represent an ideal type of endothelium for studying the site of contact of actin filaments to the plasma membrane and to the extracellular matrix in situ.

Here we show that sinus endothelial stress fibers can contract and cause changes in cellular shape. The stress fibers contain actin, myosin, α-actinin, and tropomyosin, and are composed of myosin-like filaments and actin filaments with changing polarities that are arranged in a way that might allow a sliding filament mechanism. Like stress fibers in vitro, the plasmalemmal attachment sites of the stress fibers in situ contain vinculin and, on the extracellular side, laminin, fibronectin, and collagens.

Materials and Methods

Fluorescence Microscopy

Human spleens removed surgically because of traumatic rupture, gastric cancer, or congenital spherocytosis were obtained immediately after exstirpation. Small

tissue pieces (~1 mm^3) were frozen in isopentane cooled with liquid nitrogen. Frozen tissue blocks were either used for cryosectioning or for freeze-drying and subsequent embedding in Epon as described elsewhere (16, 19–21). Cryostat sections 3–5-μm thick and 0.5–1-μm thick plastic sections of the freeze-dried and Epon-embedded tissue (from which the resin had been previously removed) were incubated with the desired antibodies using the indirect immunofluorescence technique as described (16, 21).

Sequential immunofluorescence was used to display two different antibodies in the same section. The first antibody was visualized by indirect immunofluorescence (26) and photographed. The initial staining was then eliminated by removing the immunoglobulin with 0.05% $KMnO_4$ in 0.1% H_2SO_4 for 10 s followed by exposure to 0.5% $Na_2S_2O_5$ for 5–10 s (16). After the sections had been checked for complete removal of the previous stain (which always was the case under these conditions), they were reincubated with another antibody, which again was visualized by indirect immunofluorescence.

Staining with tetramethylrhodamine isothiocyanate (TRITC)[1]-labeled phalloidin (which is a specific probe for polymerized actin, F-actin; 22) was done using cryostat sections fixed with 2% paraformaldehyde in phosphate-buffered saline (PBS) for 15 min. TRITC-phalloidin was used at a concentration of 1.4 μg/ml. Paired fluorescence with TRITC-phalloidin and antibodies was done by mixing TRITC-phalloidin with the fluorescein isothiocyanate-labeled goat anti-rabbit IgG (Miles, Frankfurt, FRG), which was used at a dilution of 1:40 in PBS.

Isolated endothelial cells were attached to glass slides coated with gelatin. The attached cells were fixed with 2% paraformaldehyde in PBS (15 min), rinsed with PBS (3× 5 min), made permeable with cold acetone (−20°C, 5 min), washed with PBS that contained 1% bovine serum albumin (BSA) (15 min), and then incubated with antibodies or TRITC-phalloidin. Cells that had been stored in 50% glycerol in buffer B (vide infra) were stained in suspension and finally spread on glass slides (mounted in 70% glycerol in PBS) for microscopic examination.

Controls were done in which the specific antibodies were replaced by (*a*) the preimmune serum in a dilution of 1:10 or (*b*) the specific antibodies absorbed with an excess of their respective antigens. Specificity of staining with TRITC-phalloidin was controlled by a 1:10 (wt/wt) mixture of TRITC-phalloidin and unlabeled phalloidin (Boehringer Mannheim GmbH, Mannheim, FRG). Under these control conditions, no staining with antibodies and TRITC-phalloidin was seen.

Antibodies, Immunoblotting

Antibodies to chicken gizzard and pectoral muscle actin and α-actinin (21), chicken gizzard vinculin (21) and tropomyosin (18), human uterine myosin (8), human platelet myosin (49) and calf thymus myosin (17), human tissue culture (skin) fibroblast vimentin (61), human serum fibronectin (54), human placental and mouse sarcoma laminin (purchased from Medac, Hamburg, FRG and obtained from Dr. Mollenhauer, Marburg), and human skin types I and III collagen (29) were prepared and checked for specificity as described in the references indicated. IgG fractions of the antisera were prepared by ammonium sulfate precipitation, gel filtration on Sephadex G 150, and ion exchange chromatography on DE 52 (Whatman, Maidstone, England).

Pellets of isolated sinus endothelium were subjected to SDS PAGE (5–15%) in the presence of 2% β-mercaptoethanol. Electrophoretically separated proteins were transferred to nitrocellulose paper (Schleicher & Schüll, Darmstadt, FRG) which was then processed for antibody staining using the peroxidase, anti-peroxidase method as described (19).

Electron Microscopy, S-1 Decoration

Small tissue pieces of the spleen were fixed overnight at 4°C with 2% glutaraldehyde in PBS, postfixed with 2% OsO_4 in PBS for 2 h, dehydrated in graded ethanol series, and embedded in Epon. Thin sections (50–100 nm) were counterstained with uranyl acetate and lead citrate and viewed with a Philips 300 electron microscope. For analysis of the polarity of actin filaments in the sinus endothelium, isolated cells were permeabilized for 5 h in a 1:1 (vol/vol) mixture of glycerol and Pipes buffer (0.1 M Pipes, 5 mM $MgCl_2$, 0.1 mM EDTA at pH 7.0). Cells were then placed in 5% glycerol and 95% Pipes buffer and incubated for 2 h with 2 mg/ml S-1 myosin subfragment in Pipes buffer. S-1 fragment was prepared from chicken pectoral muscle (51).

Control incubations were done with 2 mg/ml S-1 myosin subfragment in Pipes buffer that contained 5 mM ATP (pH 7.0). After incubation cells were rinsed with Pipes buffer (5 min). Pellets of the cells were fixed for 1 h in 2% glutaraldehyde and 0.2–2% tannic acid (5), in Pipes buffer, adjusted to pH 7.4 with NaOH. Pellets were then rinsed for 30 min in Pipes buffer, postfixed with 1% OsO_4 in cacodylate buffer (pH 6.0) for 1 h, followed by block staining in 1% aqueous uranyl acetate (1 h), dehydration in alcohol, and embedding in Epon.

Isolation of Endothelial Cells

All steps were done at 4°C. Splenic tissue was extensively minced and teased with tweezers and razor blades and suspended for 30–60 min in buffer A (96 mM NaCl, 8 mM KH_2PO_4, 5.6 mM Na_2HPO_4, 1.5 mM KCl, 10 mM EDTA at pH 6.8). After gentle agitation and continuous passage through a Pasteur pipette, detached cells were filtered through a 200-μm mesh nylon cloth and collected at 400 *g* for 10 min. The pellet consisted mainly of red blood cells, white blood cells, platelets, and a rather small proportion of sinus endothelial cells. Treatment of minced tissue with 0.05% collagenase or 0.1% trypsin led within a few minutes to the formation of a sticky gel-like substance that prevented any separation of the cells.

Sinus endothelial cells were separated from blood cells by centrifugation on Percoll Hypaque (Pharmacia, Uppsala, Sweden). 1 ml of pelleted cells suspended in 1.073 g/ml Percoll in PBS were layered underneath the following Percoll solutions in isotonic PBS: 1 ml of density 1.060 g/ml, 1 ml of 1.047 g/ml, 1 ml of 1.035 g/ml, and 1 ml of 1.022 g/ml. After centrifugation at 100 *g* for 30 min, the fraction collected from the interphase between steps of density 1.047/1.035 g/ml contained isolated sinus endothelial cells at high purity.

Contraction Studies

Contraction studies were done at room temperature. Isolated endothelial cells were suspended in buffer B that contained 100 mM KCl, 3 mM $MgCl_2$, 3 mM EGTA, 10 mM imidazole (or 10 mM sodium phosphate) pH 6.9 (7). Samples of endothelial cells were permeabilized by (*a*) 30-min exposure to 0.2% Triton X-100 in buffer B (4°C) or (*b*) by 3 h (4°C) up to several days (−15°C) exposure to 50% glycerol in buffer B. The cells were then washed with buffer B and exposed to buffer B that contained 0.5–2 mM ATP (contraction solution). In some experiments, 3 mM $CaCl_2$ (prepared from an ion standard solution; Fluka, Switzerland) was added to the contraction solution. The free Ca^{2+} concentration of this solution has been calculated to be 1×10^{-5} M (7). Control experiments were done in which ATP was replaced by 1–5 mM pyrophosphate, AMP, ADP, or the ATP analogues AMP-PNP and AMP-PCP (Boehringer Mannheim GmbH). Cells were incubated in test tubes with contraction solution or the various control solutions and were then placed on slides for microscopic examination (test tube assay). For direct examination of cellular changes, the space between the slide and coverslip was perfused with contraction solution or the corresponding control solutions. In some instances, individual cells could be examined by incubating first with the various control solutions and finally with contraction solution.

Results

Morphology of Isolated Endothelial Cells

The cell fraction collected from the interface between steps of density 1.047/1.035 g/ml Percoll Hypaque contained isolated sinus endothelial cells at high purity (Fig. 1). Contamination with some free nuclei and few stellate-shaped reticular cells (parasinusoidal or cordal cells) was negligible. The isolated endothelial cells showed the typical features of their in situ morphology which clearly distinguished them from all other cell types of the spleen: The cells were rod-shaped (up to 80-μm long) with a bulging perinuclear area. Almost all cells were characterized by periodically arranged groove-like incisures. These incisures represent the sites where the belt-like formations of the basement membrane, the argyrophilic ring fibers, are inserted in the basal cell surface (see Figs. 3 and 26). The distance between adjacent ring fiber grooves in cells in situ is 2–4 μm (35, and unpublished observations), which is exactly the distance found between adjacent incisures in isolated cells.

1. *Abbreviation used in this paper:* TRITC, tetramethylrhodamine isothiocyanate.

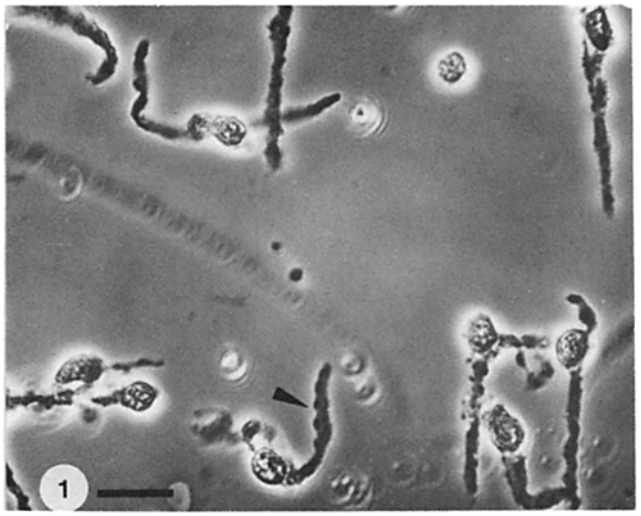

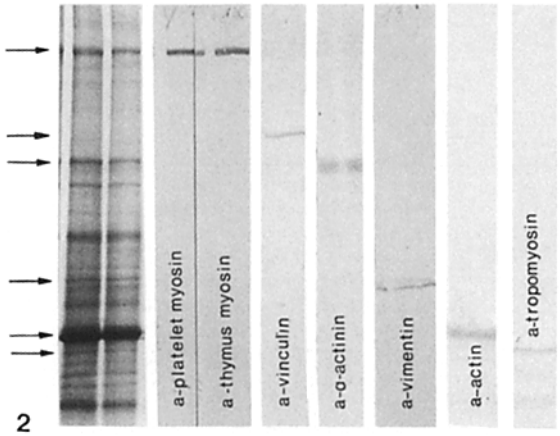

Figures 1 and 2. (Fig. 1) Phase contrast micrograph of isolated sinus endothelial cells. Note the rod-shaped morphology and the characteristic bulging segments (arrowhead). Bar, 10 μm. (Fig. 2) Separated proteins of isolated sinus endothelial cells (Fig. 1) transferred to nitrocellulose paper and labeled with the antibodies indicated. In Coomassie Blue–stained lanes (left two lanes), protein bands corresponding to antibody-labeled bands are indicated by arrows. Actin-, myosin-, and α-actinin-containing polypeptide bands are major components of the sinus endothelium.

Immunoblotting Studies

Proteins of isolated sinus endothelial cells were separated by SDS PAGE and transferred to nitrocellulose paper (Fig. 2). Immunolabeling of the blotted gels revealed distinct polypeptide bands specifically labeled with antibodies to myosin (M_r ~200,000), vinculin (M_r ~130,000), α-actinin (M_r ~100,000), vimentin (M_r ~55,000), actin (M_r ~42,000), and tropomyosin (M_r~ 36,000). No other cross-reactive polypeptide bands were detected.

Ultrastructure of Stress Fibers

The overall fine structural organization of the cytoskeleton in the human sinus endothelium was largely consistent with previous descriptions dealing with the sinus endothelium in the human (11, 35) and rat (13) spleen (see Fig. 26). Arrays of parallel-aligned stress fibers were strictly confined to the cellular segments interposed between adjacent extracellular matrix contacts. The most prominent stress fibers (up to 0.4 μm in diameter) extended underneath the basolateral plasma membrane which borders on the interendothelial slits (not shown). In longitudinal and transverse sections of stress fibers in glycerol-extracted cells, two types of filaments were seen (Figs. 3 and 4): (*a*) microfilaments with a diameter of 5–7 nm, and (*b*) thicker filaments, ~10–15 nm in diameter and 150–300-nm long (Fig. 4, *A* and *B*). The ends of many of these myosin-like filaments appeared to splay (Fig. 4*B*) into finer subfilaments. The thin actin-like filaments were frequently observed in parallel alignment with the myosin-like filaments (Fig. 4*B*). The distance between thin and thick filaments was frequently as close as 10–20 nm (Fig. 4*B*), which is about the space observed between actin filaments and the surface of myosin filaments in striated muscle (60).

S-1 Myosin Subfragment Decoration

Microfilaments of endothelial stress fibers were identified as actin-containing filaments by their affinity for myosin subfragments S-1. Myosin fragments formed typical arrowhead complexes along the actin filaments, which allowed the visualization of actin filaments of opposite polarities (Figs. 6 and 7). At the plasmalemmal attachment site of stress fibers, located at both sides of the ring fiber grooves, actin filaments terminated in aggregates of electron-dense material. In favorable planes of sections, the attached filaments displayed a uniform polarity with the arrowheads pointing away from the attachment site (Figs. 5*B* and 7).

Immunohistochemistry

Cytoskeleton. In tissue sections (Figs. 8–12), fluorescent phalloidin and antibodies to actin, myosin, tropomyosin, and α-actinin displayed a strong affinity for the arrays of stress fibers located in the basal portions of the sinus endothelium (individual stress fibers can be seen in Figs. 9*A*, 10, 11, 17, and 18). Antibodies to α-actinin differed from all other antibodies in producing an interrupted immunostain of the stress fibers which was most clearly seen in semithin (0.5 μm) sections of quick-frozen, freeze-dried, and plastic-embedded tissue. As a rule, 4–6 fluorescent dots were observed along individual stress fibers extending between adjacent extracellular matrix contacts.

At regular intervals of 4–6 μm, the arrays of stress fibers were interrupted by unstained transverse bands 0.5–1-μm wide. These intersections exactly corresponded to the sites of contact of endothelial cells with the ring fibers as determined by simultaneous staining of the same sections with both antibodies to contractile proteins and to fibronectin (Figs. 8 and 9). As seen in Figs. 12 and 19, these sites of stress fiber-to-membrane and membrane-to-extracellular matrix association were brightly labeled with antibodies to vinculin (pairs of fluorescent dots in cross-section and pairs of stripes in tangential sections of ring fibers).

Isolated sinus endothelial cells (Figs. 17–20) displayed a virtually identical distribution of actin, myosin, α-actinin, tropomyosin, and vinculin as seen in tissue sections. The cytoplasm overlying the ring fiber grooves was unstained and appeared as nonfluorescent transverse bands (surface view) or gaps (lateral view). Ocassionally individual stress fibers were revealed that showed a continuous fluorescence with phalloidin and antibodies to actin. Antibodies to myosin and α-

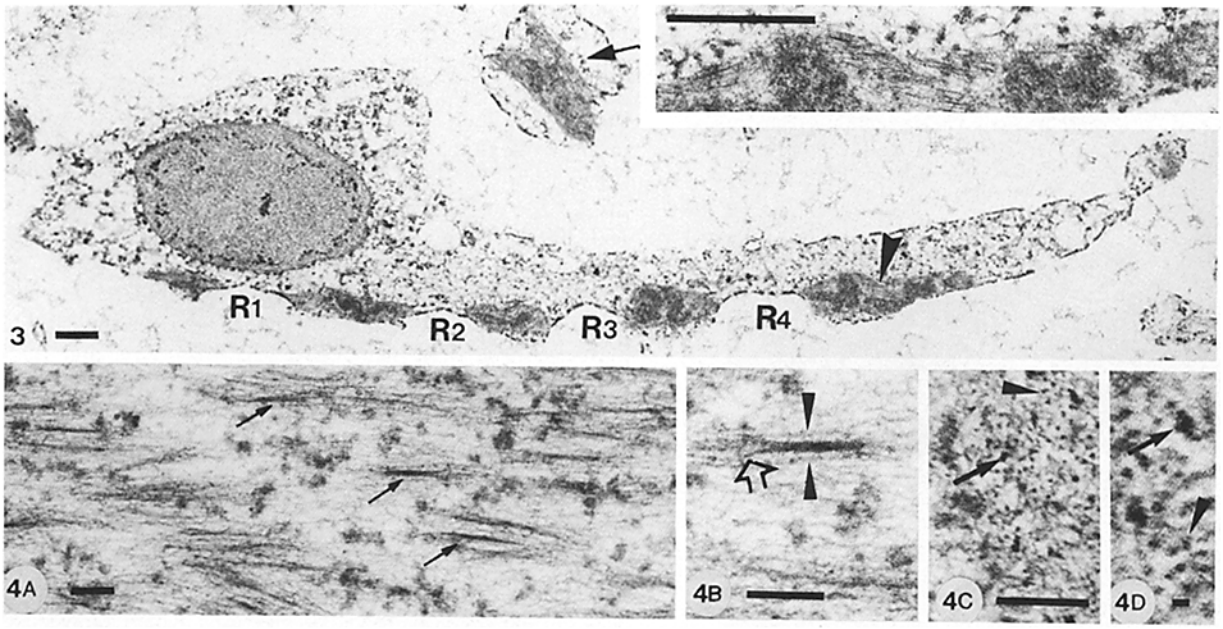

Figures 3 and 4. (Fig. 3) Longitudinal sections of a glycerol-extracted isolated endothelial cell. R_1–R_4 denote grooves located at the former sites of contact with ring fibers in situ. Arrow points to tangentially sectioned stress fibers. Arrowhead indicates the area shown in the inset at higher magnification. Bars, 1 μm. (Fig. 4) Longitudinal (*A* and *B*) and transverse (*C* and *D*) sections of stress fibers of glycerol-extracted cells showing thin actin-like filaments (arrowheads) and thicker myosin-like filaments (arrows). Large arrow in *B* points to splaying head portion of a myosin-like filament. Bars: (*A–C*) 100 nm; (*D*) 10 nm.

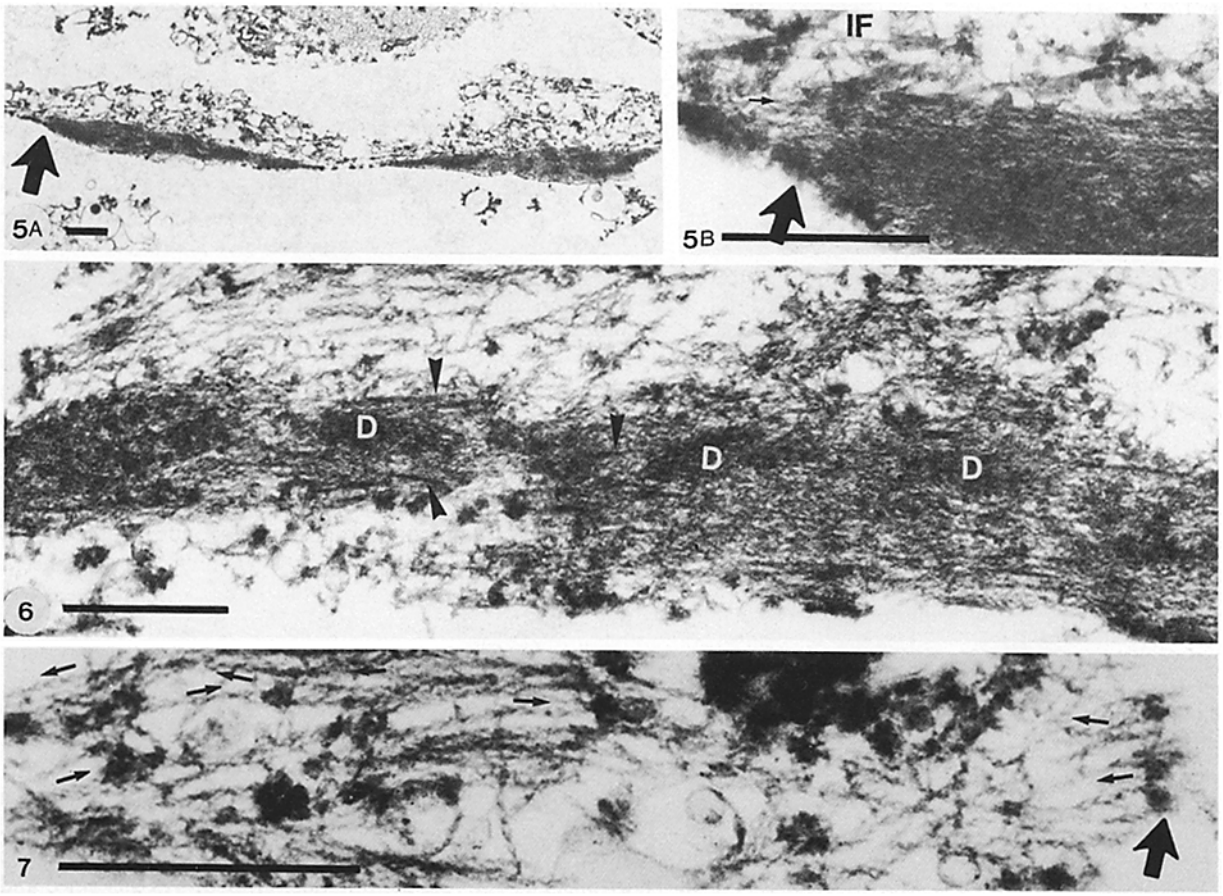

Figures 5–7. S-1 fragment decoration of actin filaments in sinus endothelial stress fibers. Stress fibers are composed of actin filaments with changing polarities (indicated by small arrows, Fig. 5*B* and 7). Thick arrows in Figs. 5 and 7 point to dense material associated with the plasmalemmal attachment site of the stress fibers. At these sites actin filaments are uniformly polarized with the arrowheads pointing away from the membrane. In Fig. 7 stress fiber densities (*D*) and myosin-like filaments (arrowheads) are seen. Bars: (5 *A*) 1 μm; (5 *B*–7) 0.5 μm.

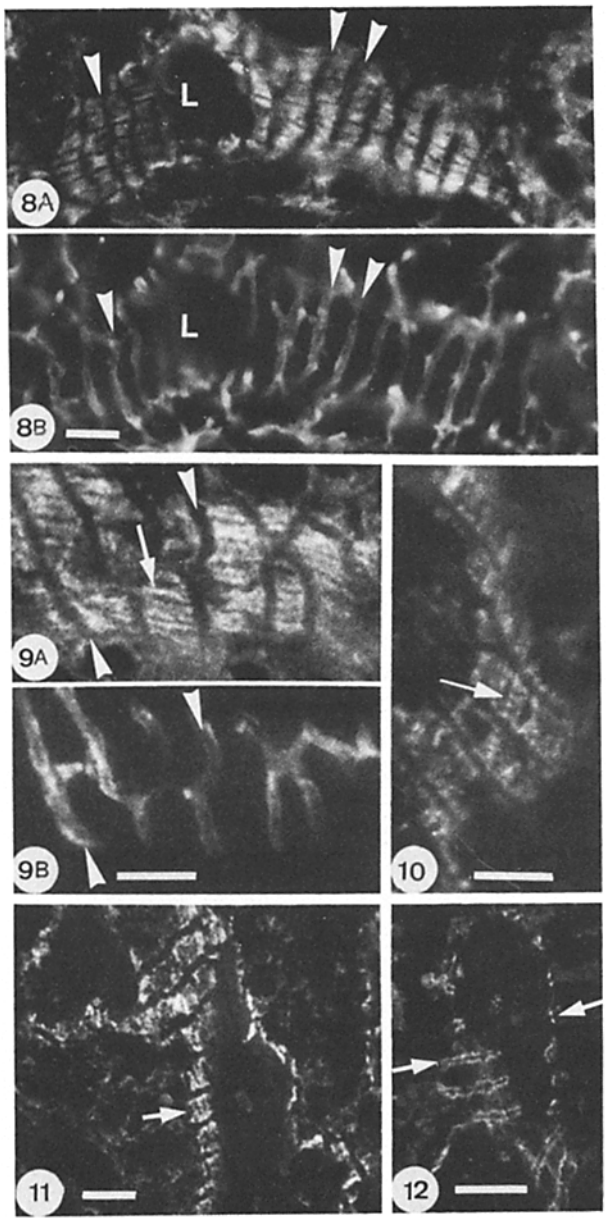

Figures 8–12. Frozen section (Fig. 8, *A* and *B*) and semithin plastic sections (Figs. 9–12) of the sinus wall stained with rhodamine phalloidin (Fig. 8*A*) and antibodies to fibronectin (Figs. 8*B* and 9*B*), myosin (Fig. 9*A*), α-actinin (Fig. 10), tropomyosin (Fig. 11), and vinculin (Fig. 12). Double-labeling of the same sections with antibodies to fibronectin (Figs. 8*B* and 9*B*) and rhodamine-phalloidin (Fig. 8*A*) and anti-myosin (Fig. 9*B*) demonstrate that the stress fibers are confined to the cellular segments interposed between the fibronectin-containing ring fibers (arrowheads point to individual ring fibers; *L* marks the sinus lumen). Individual stress fibers are well seen in Figs. 9*A*, 10, and 11 (arrows). Anti-vinculin (Fig. 12) stains the plasmalemmal attachment site of the stress fibers located at the surface of the ring fibers (pairs of strips in tangential and pairs of dots in transverse sections of the ring fibers, arrows). Bars, 10 μm.

actinin, however, often caused an interrupted fluorescence of the stress fibers (Fig. 17). Immunostain specific for vinculin was confined to the stress fiber termini located at both sides of the ring fiber grooves (Fig. 19). Antibodies to the intermediate filament protein vimentin stained the endothelial cells along their whole length without any interruptions (Figs. 13 and 20). This pattern correlates well with the ultrastructural distribution of intermediate filaments which were found throughout the whole length and cross-sectional profile of the cells (reference 11, and unpublished observations).

Extracellular Matrix. Ring fibers displayed a strong affinity for antibodies to laminin, fibronectin, and to type I and type III collagen (antibodies to types IV and V collagen were not tested). Laminin immunoreactivity (Fig. 14) was confined to a delicate zone located at the very periphery of the ring fibers (closest to the cell surface). Anti-fibronectin fluorescence (Figs. 8 and 9) was also concentrated in the periphery of the ring fibers but in a broader zone as compared with anti-laminin. Types I and III collagens (Figs. 15 and 16) were located throughout the whole cross-sectional profile of ring fibers, with still some preference for their periphery. Staining intensity seen with anti-type III collagen was considerably stronger than that observed with anti-type I collagen.

Contraction Studies. When suspensions of permeabilized cells were exposed to 0.5 or 1 mM ATP in buffer A (absence of Ca^{2+}), virtually all endothelial cells displayed typical morphological changes (Figs. 21–23) which were characterized by (*a*) formation of bulging segments along the abluminal cellular surface (serrated appearance) and (*b*) different degrees of shortening of the cells. This ATP-induced contraction and segmental bulging started within a few seconds after addition of ATP and was completed within a period of 1–3 min. No cellular changes were observed when ATP was replaced by 1–5 mM pyrophosphate (Fig. 23*B*), AMP, ADP, or the ATP analogues AMP-PNP and AMP-PCP. Moreover, no changes occurred in the absence of Mg^{2+} (5 mM EDTA). Quite in contrast to endothelial cells, skeletal muscle myofibrils (routinely added to the suspension of endothelial cells as an internal biological standard) did not contract in response to Mg^{2+} ATP and, expectedly, needed addition of micromolar concentrations of Ca^{2+} for shortening. To determine whether the ATP-induced morphological changes of endothelial cells were caused by contraction of stress fibers, cells were labeled with fluorescent phalloidin and were then examined by fluorescence microscopy before and after addition of ATP (phalloidin at 1.4 μg/ml did not inhibit contraction of both stress fibers and myofibrils). As shown in Figs. 24 and 25, cellular shortening and segmental bulging was clearly correlated with shortening of stress fibers. Thus, these changes in cellular shape and length have to be considered as motile events mediated by contraction of stress fibers.

Discussion

Molecular Structure of Stress Fibers

Like stress fibers in cultured cells (5, 55), endothelial stress fibers in situ were composed of actin filaments in parallel alignment with non-uniform polarity. Often actin filaments with opposite polarities were seen in close proximity. In addition to actin filaments, the stress fibers contained numerous thicker (10–15 nm) and shorter (200–300 nm) filaments, the dimensions and morphology of which are similar to filaments formed from myosin isolated from a variety of nonmuscle cells (2, 48, 49, 56, 68). Like myosin filaments in vitro, endothelial myosin-like filaments appeared to splay into finer subfilaments most probably representing parts of indi-

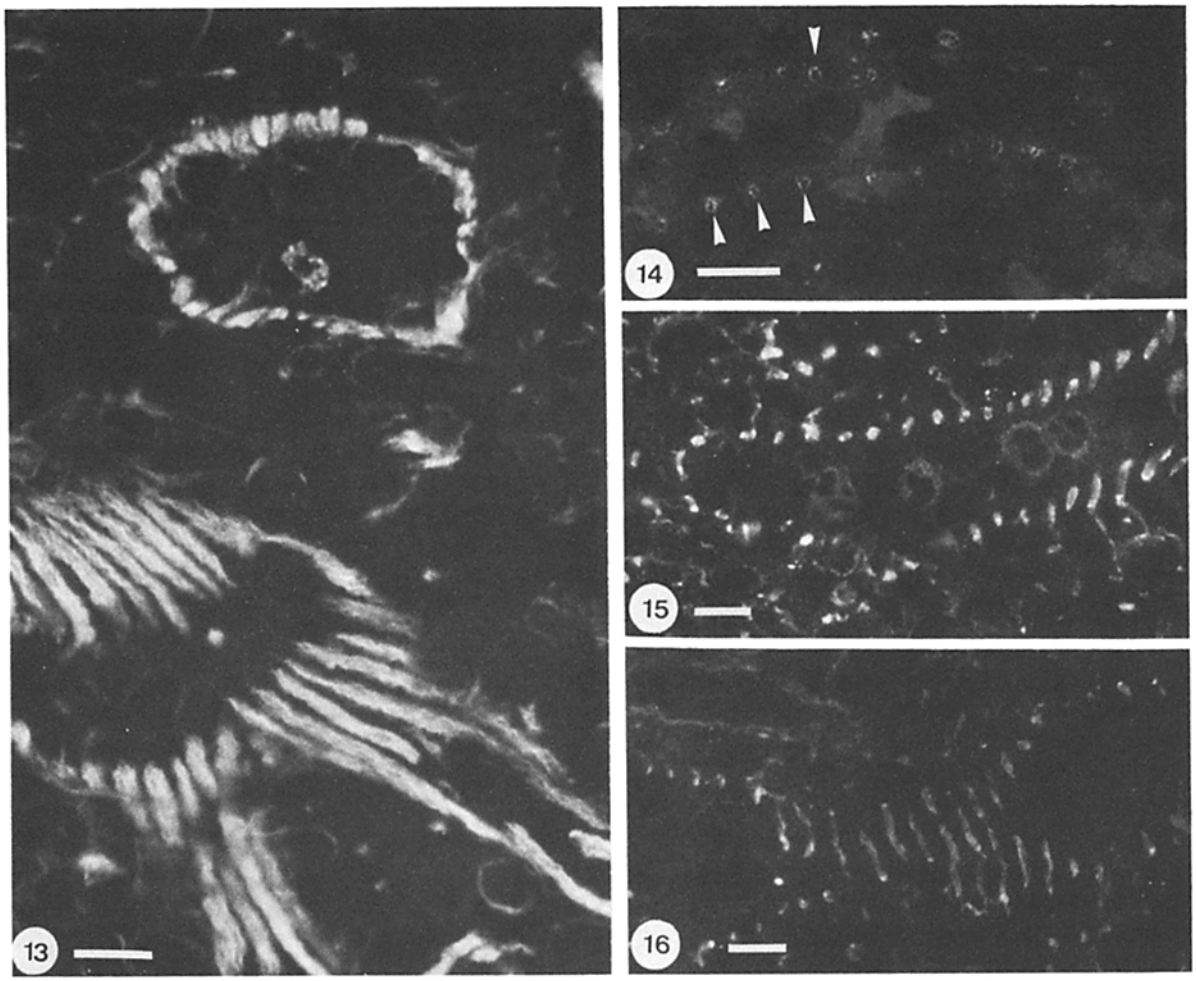

Figures 13–16. (Fig. 13) Immunostaining specific for vimentin extends throughout the whole profile and length of the sinus endothelial cells. Bar, 10 μm. (Figs. 14–16) Localization of components of the extracellular matrix (for fibronectin see Figs. 8 *B* and 9 *B*). Anti-laminin (Fig. 14) is confined to the very periphery of ring fibers (arrowheads), while collagens type III (Fig. 15) and type I (Fig. 16) extend more into the cores of ring fibers (1-μm plastic section). Bars, 10 μm.

vidual myosin molecules. In SDS PAGE of isolated endothelial cells, the protein band that contained the myosin heavy chains was the most prominent protein band next to the actin-containing band. This finding correlates well with the rather high density of thick myosin-like filaments observed in sections of both well-fixed spleen tissue (reference 14, and unpublished observations) and glycerol-extracted, isolated cells. The present observation in endothelial stress fibers of longitudinally arranged myosin-like filaments located within arrays of actin filaments with opposing polarity strongly supports the general assumption that stress fibers create tension by a sliding filament mechanism (32, 39, 55) related to muscle contraction (60) (Fig. 26). Myosin-like filaments have previously not been demonstrated convincingly in any kind of stress fiber. The only indication of the existence of a population of thicker and shorter filaments (17 × 250 nm) in stress fibers was obtained in HeLa cells permeabilized with saponin in the presence of glutaraldehyde and tannic acid (46). Recently, bipolar myosin-like filaments have also been shown in the circular contractile ring of the intestinal brush border (36).

In the majority of cells, antibodies against myosin (and tropomyosin) did not produce the typical, interrupted sarcomere-like staining pattern known from stress fibers in aortic endothelium in situ (65) and most cell types in vitro (31, 33, 50, 63). This is probably due to two reasons. First, the myosin-containing segments might optically overlap in these rather thick ribbon-shaped arrays of stress fibers, so that only occasionally an interrupted staining pattern was seen (Fig. 17). Second, in most stress fibers of glycerol-extracted cells, myosin-like filaments displayed a more or less even distribution throughout the whole length of the fibers without any obvious segmental arrangement (Fig. 6). This is also the case in the contractile ring that extends along the zonula adherens of epithelial cells (36). In contrast to the myosin-like immunostain, antibodies to α-actinin produced a characteristic interrupted staining pattern seen along numerous stress fibers. Similar interruptions are well-known from α-actinin in stress fibers of cultured cells (43) and most probably result from a selective affinity of α-actinin antibodies for the stress fiber densities (40).

Stress Fiber–Membrane Association

The well-defined sites of contact of sinus endothelial stress fibers to the plasma membrane allowed a detailed analysis of the stress fiber–membrane association in situ. At the plasmalemmal termination site, virtually all filaments had the

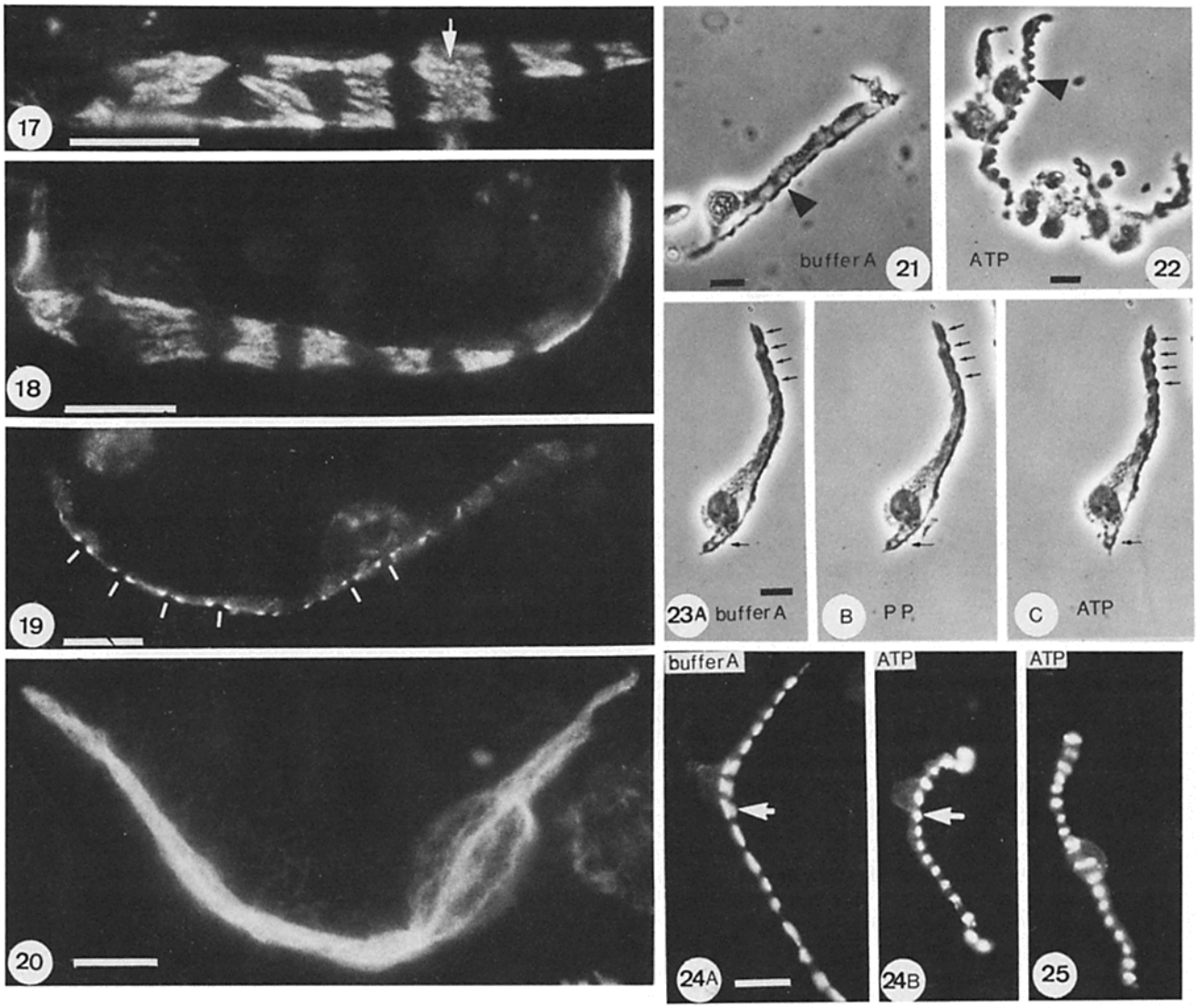

Figures 17–25. (Figs. 17–20) Distribution of myosin (Fig. 17), actin (Fig. 18), vinculin (Fig. 19), and vimentin (Fig. 20) in isolated sinus endothelial cells. Each fluorescent segment in Figs. 17 and 18 is composed of arrays of stress fibers. The arrow in Fig. 17 points to interruptions seen along some of the stress fibers. The unstained transverse bands correspond to the extracellular matrix contacts of the cells (ring fibers). Vinculin (Fig. 19) is concentrated at the termination site of stress fibers located at both sides of the ring fiber grooves (dashes). Intermediate filaments, visualized by anti-vimentin (Fig. 20), extend throughout the entire length of the cells without any interruptions. Bars, 10 μm. (Figs. 21–23) Phase contrast micrographs of isolated endothelial cells permeabilized with 50% glycerol in buffer A. Note distinct ATP-induced changes in cellular shape (bulging segments) and length (arrows and arrowheads). Pyrophosphate (*PP*) has no visible effect (for further control experiments refer to text). Bars, 10 μm. (Figs. 24 and 25) Effect of MgATP on stress fibers visualized by pre-labeling of stress fibers with rhodamine-phalloidin. MgATP-induced shortening of the cells is accompanied by shortening of stress fibers (arrow). Bars, 10 μm.

same orientation with the arrowhead complexes of the bound myosin fragments pointing away from the plasma membrane. A similar polarity of actin filaments has been previously described for other types of actin filament–membrane associations (5, 42). Like stress fibers in vitro, both vinculin and α-actinin were found concentrated at the plasmalemmal termination site of sinus endothelial stress fibers, which thus appear to be closely related to focal adhesion plaques of cells in tissue culture (30, 45).

Relation to Components of the Extracellular Matrix

Studies mainly performed on cells in vitro indicate that the cytoskeleton and the extracellular matrix are part of a continuous supramolecular assemblage (9, 34, 37, 57, 66). A major component of the extracellular matrix is fibronectin, a multifunctional glycoprotein that interacts with other structural molecules such as collagen, glycosaminoglycans, and with components of the cell surface (for review, see reference 53). Controversial results were obtained regarding the occurrence of fibronectin at focal contacts (adhesion plaques) of cultured cells (3, 4, 6, 12, 23, 37, 41, 57, 58). As demonstrated in this paper, antibodies to fibronectin displayed a selective affinity for the focal contact–like termination site of endothelial stress fibers and appeared to be absent from the remaining cell surface. Thus, sinus endothelial cells of the spleen represent an example of a cell in situ in which fibronectin is concentrated at the extracellular side of the stress fiber termini as is probably also true of another cell type in situ, i.e., the myofi-

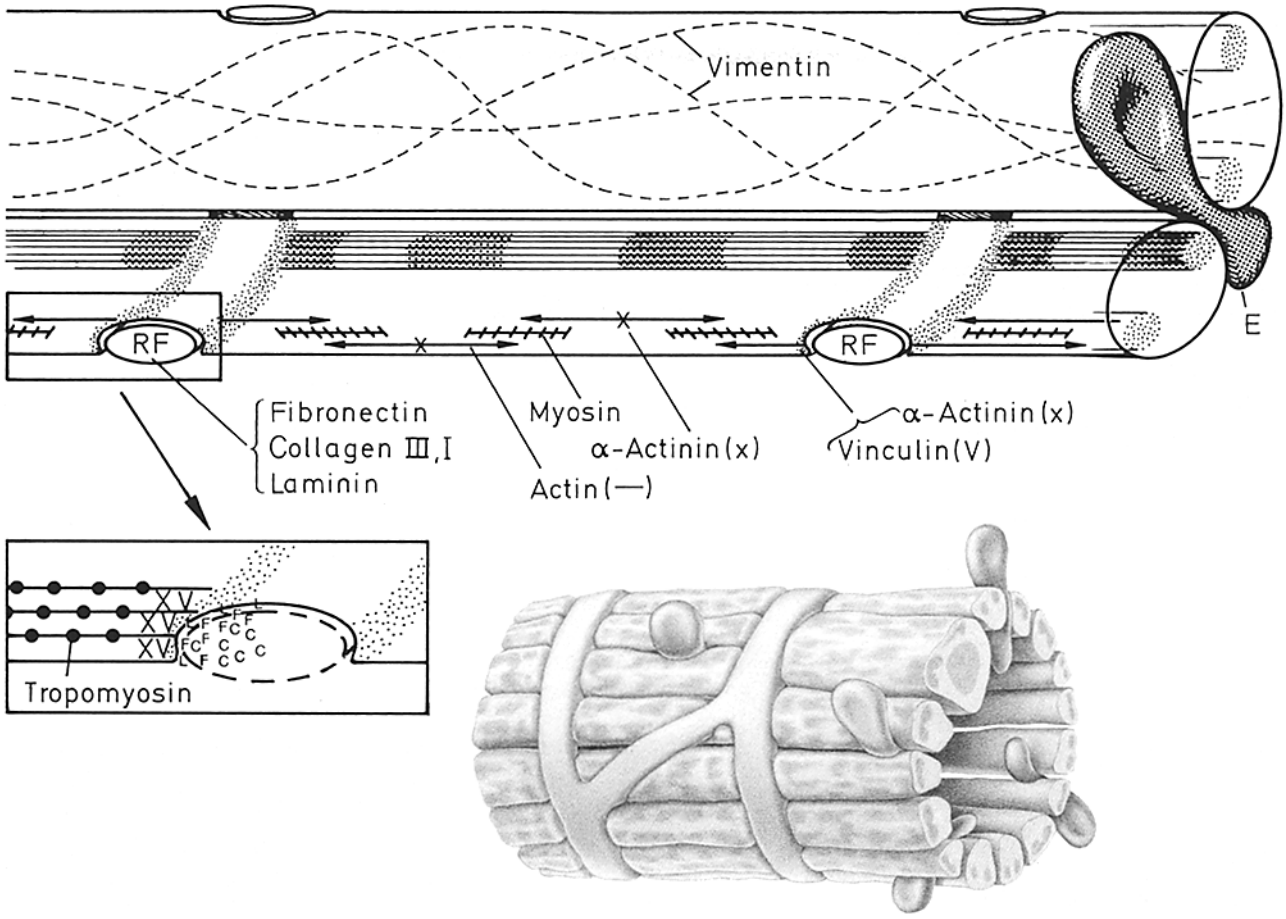

Figure 26. Schematic drawing of the human splenic sinus wall. Stress fibers are most pronounced along either side of the intercellular slits which are the sites of erythrocyte (*E*) passage. End-on, the stress fibers are attached to the plasma membrane at places where the belt-like formations of the basement membrane (ring fibers, *RF*) abut the endothelium. Tonofilaments of the vimentin type extend throughout the whole length and profile of the cells. The cell-to-extracellular matrix contacts represent focal-contact–like complexes with vinculin (*V*) and α-actinin (*X*) at the cytoplasmic face, and laminin (*L*), fibronectin (*F*), and collagens (*C*) at the extracellular face (for further details refer to text).

broblast of granulation tissue (59). These findings show that it is sometimes difficult to generalize observations made in vitro, which in several cases indicated the absence of fibronectin from focal adhesion plaques (3, 4, 6, 12, 23). In addition to fibronectin, the extracellular aspect of the site of contact of the sinus endothelium to the extracellular matrix (i.e., the ring fibers) was characterized by laminin-like immunostaining, which appeared to be located in a very narrow zone close to the cell surface. Since the basal lamina of sinus endothelial cells is confined to the ring fibers ("annular component of the basement membrane", 11), laminin, a major glycoprotein of basal laminae, was to be expected at this site. Laminin is thought to promote the binding of the cell membrane to the basement membrane and to link various macromolecules in the extracellular matrix (62). Type III collagen and fibronectin, both of which have been shown previously to be associated with the stroma of lymphatic tissue (29, 53), have to be considered as major components of the reticular ("argyrophilic") fibers in the human spleen.

Requirements for Contraction

Stress fiber–containing cellular portions (38) and individual stress fibers (39) of cultured fibroblasts have been shown to contract in response to Ca^{2+} and ATP. Contraction of stress fibers in isolated sinus endothelial cells of the spleen required ATP but was independent of Ca^{2+}. Although we cannot exclude the possibility of any kind of in vitro effect responsible for this independence of Ca^{2+}, it is interesting to note in this context that capillary and venular permeability (which is thought to be regulated by interendothelial gap formation) could be induced by ionophore A 23187 independent of Ca^{2+} entry (47). If interendothelial gap formation is produced by an actomyosin-like mechanism (actin and myosin are strategically located along the junctional plasma membrane of these cells; 14), then this kind of actomyosin-mediated cell motility might be accomplished independent of Ca^{2+}, as is the contraction of stress fibers in glycerol-extracted endothelial cells of the splenic sinus.

Functional Implications of Endothelial Stress Fibers

Stress fiber–containing endothelial cells tend to be located at sites in the vascular system exposed to high levels of shear force of blood flow, i.e., in endothelial cells of arteries and chambers of the heart (14, 65, 67), in bulging endothelial cells at branchings of capillaries (1, 44, 64), and as shown here, in the sinus endothelium of the mammalian spleen. Although the splenic sinus endothelium is part of the microcirculatory system, it is probably also exposed to particular levels of shear

forces: The interendothelial slits located between the rod-shaped sinus endothelial cells are the critical sites in the body to filter out damaged or abnormal red cells from circulation (11). Blood cells and plasma, which enter the extravasal space of the spleen via terminally open blood vessels, are permanently pushed through the interendothelial slits into the sinus lumen. The resulting shear forces probably require particular cellular support by stress fibers, which may stabilize the margins of the interendothelial slits and may help to prevent cellular detachment.

In view of our previous observation that endothelial stress fibers can be induced experimentally by exposure of endothelial monolayer cultures to arterial levels of fluid shear stress (24), it is most likely that contractility of stress fibers serves to apply isometric tension, which allows the cells to withstand the shear forces and to remain firmly attached to the substratum.

We are grateful to Dr. S. Gay (Birmingham, AL), Dr. J. Dieckhoff (Marburg), Dr. U. Gröschel-Stewart (Darmstadt), and Dr. J. Mollenhauer (Marburg) for providing antibodies to the extracellular matrix proteins and to human uterine myosin. F. Fiebiger (Marburg) kindly made the drawings presented in Fig. 26.

This work was supported by the Deutsche Forschungsgemeinschaft (Dr 91-4-1, 91-4-3).

Received for publication 26 November 1985, and in revised form 16 January 1986.

References

1. Addicks, K., H. Weigelt, G. G. Hauck, D. W. Lübbers, and H. Knoche. 1979. Light- and electronmicroscopic studies with regard to the role of intraendothelial structures under normal and inflammatory conditions. *Bibl. Anat.* 17:32–35.

2. Adelstein, R. S., M. A. Conti, G. S. Johnson, I. Pastan, and T. D. Pollard. 1972. Isolation and characterization of myosin from cloned mouse fibroblast. *Proc. Natl. Acad. Sci. USA.* 69:3693–3697.

3. Avnur, Z., and B. Geiger. 1981. The removal of extracellular fibronectin from areas of cell-substrate contact. *Cell.* 25:121–132.

4. Badley, R. A., A. Woods, C. G. Smith, and D. A. Rees. 1980. Actomyosin relationship with surface features in fibroblast adhesion. *Exp. Cell Res.* 126:263–272.

5. Begg, D. A., R. Rodewald, and L. I. Rebhun. 1978. The visualization of actin filament polarity in thin sections. Evidence for the uniform polarity of membrane-associated filaments. *J. Cell Biol.* 79:846–852.

6. Birchmeier, C., T. E. Kreis, H. M. Eppenberger, K. H. Winterhalter, and W. Birchmeier. 1980. Corrugated attachment membrane in WI-38 fibroblasts. Alternating fibronectin fibers and actin-containing focal contacts. *Proc. Natl. Acad. Sci. USA.* 77:4108–4112.

7. Burgess, D. R., and B. E. Prum. 1980. Reevaluation of brush border motility: calcium induces core filament solation and microvillar vesiculation. *J. Cell Biol.* 94:97–107.

8. Burkl, B., Ch. Mahlmeister, U. Gröschel-Stewart, J. Chamley-Campbell, and G. R. Campbell. 1979. Production of specific antibodies to contractile proteins and their use in immunofluorescence microscopy. III. Antibody against human uterine smooth muscle myosin. *Histochemistry.* 60:135–143.

9. Burridge, K., and J. Feramisco. 1980. Microinjection and localization of a 130k protein in living fibroblasts: a relationship to actin and fibronectin. *Cell.* 19:587–595.

10. Byers, H. R., and K. Fujiwara. 1982. Stress fibers in cells in situ: immunofluorescent visualization with anti-actin, anti-myosin, and anti-alpha-actinin. *J. Cell Biol.* 93:804–811.

11. Chen, L.-T., and L. Weiss. 1973. The role of the sinus wall in the passage of erythrocyte through the spleen. *Blood.* 41:529–537.

12. Chen, W.-T., and S. J. Singer. 1982. Immunoelectron microscopic studies of the sites of cell-substratum and cell-cell contacts in cultured fibroblasts. *J. Cell Biol.* 95:205–222.

13. De Bruyn, P. P. H., and Y. Cho. 1974. Contractile structures in endothelial cells of splenic sinusoids. *J. Ultrastruct. Res.* 49:24–33.

14. Drenckhahn, D. 1983. Cell motility and cytoplasmic filaments in vascular endothelium. *Prog. Appl. Microcirc.* 1:55–70.

15. Drenckhahn, D., J. Dieckhoff, H.-G. Mannherz, and J. Wagner. 1984. Cytoskeleton and its relation to the extracellular matrix in the sinus endothelium of the human spleen. *Drug Res.* 34:744–745

16. Drenckhahn, D., and H. Franz. 1986. Identification of actin, alpha-actinin, and vinculin-containing plaques at the lateral membrane of epithelial cells. *J. Cell Biol.* 102:1843–1852.

17. Drenckhahn, D., U. Gröschel-Stewart, J. Kendrick-Jones, and J. J. Scholey. 1983. Antibody to thymus myosin: its immunological characterization and use for immunocytochemical localization of myosin in vertebrate non-muscle cells. *Eur. J. Cell Biol.* 30:100–111.

18. Drenckhahn, D., and U. Gröschel-Stewart. 1980. Localization of myosin, actin, and tropomyosin in rat intestinal epithelium: immunohistochemical studies at the light and electron microscope levels. *J. Cell Biol.* 86:475–482.

19. Drenckhahn, D., H.-D. Hofmann, and H.-G. Mannherz. 1983. Evidence for the association of villin with core filaments and rootlets of intestinal epithelial microvilli. *Cell Tissue Res.* 228:409–414.

20. Drenckhahn, D., J. Kellner, H.-G. Mannherz, U. Gröschel-Stewart, J. Kendrick-Jones, and J. Scholey. 1982. Absence of myosin-like immunoreactivity in stereocilia of cochlear hair cells. *Nature (Lond.).* 300:531–532.

21. Drenckhahn, D., and H.-G. Mannherz. 1983. Distribution of actin and the actin-associated proteins myosin, tropomyosin, alpha-actinin, vinculin, and villin in rat and bovine exocrine glands. *Eur. J. Cell Biol.* 30:167–176.

22. Faulstich, H., H. Trischmann, and D. Mayer. 1983. Preparation of tetramethylrhodaminyl-phalloidin and uptake of the toxin into short-term cultured hepatocytes by endocytosis. *Exp. Cell Res.* 144:73–82.

23. Fox, C. H., M. H. Cottler-Fox, and K. Yamada. 1980. The distribution of fibronectin in attachment sites of chick fibroblasts. *Exp. Cell Res.* 130:477–481.

24. Franke, R. P., M. Grafe, H. Schnittler, D. Seiffge, C. Mittermayer, and D. Drenckhahn. 1984. Induction of human vascular endothelial stress fibres by fluid shear stress. *Nature (Lond.).* 307:648–649.

25. Fujita, T. 1974. A scanning electron microscope study of the human spleen. *Arch. Histol. Jpn.* 37:187–216.

26. Gabbiani, G., M. C. Badonell, and G. Rona. 1975. Cytoplasmic contractile apparatus in aortic endothelial cells of hypertensive rats. *Lab. Invest.* 32:227–234.

27. Gabbiani, G., G. Elemer, C. Guelpa, M. B. Valloton, M. C. Badonell, and I. Huttner. 1979. Morphological and functional changes of the aortic intima during experimental hypertension. *Am. J. Pathol.* 96:399–414.

28. Gabbiani, G., F. Gabbiani, D. Lombardi, and S. M. Schwartz. 1983. Organization of actin cytoskeleton in normal and regenerating endothelial cells. *Proc. Natl. Acad. Sci. USA.* 80:2361–2364.

29. Gay, S., and T. F. Kresina. 1982. Immunological disorders of collagen. *In* Collagen in Health and Disease. M. I. V. Jayson and J. B. Weiss, editors. Chirchill Livingston, Edinburg. 269–288.

30. Geiger, B. 1983. Membrane-cytoskeleton interaction. *Biochim. Biophys. Acta.* 737:305–341.

31. Goldman, R. D., A. Milsted, J. A. Schloss, J. Starger, and M. J. Yerna. 1979. Cytoplasmic fibres in mammalian cells. *Annu. Rev. Physiol.* 41:703–722.

32. Gordon, W. E. 1978. Immunofluorescent and ultrastructural studies of "sarcomeric" units in stress fibres of cultured non-muscle cells. *Exp. Cell Res.* 117:253–260.

33. Gröschel-Stewart, U., and D. Drenckhahn. 1982. Muscular and cytoplasmic contractile proteins-biochemistry, immunology, structural organization. *Collagen Relat. Res.* 2:381–463.

34. Heggeness, M. H., J. F. Ash, and S. J. Singer. 1978. Transmembrane linkage of fibronectin to intracellular actin-containing filaments in cultured human fibroblasts. *Ann. N. Y. Acad. Sci.* 312:414–417.

35. Heusermann, U., and H. J. Stutte. 1975. Comparative histochemical and electron microscopic studies of the sinus and venous walls of the human spleen with special reference to the sinus-venous connections. *Cell Tissue Res.* 163:519–533.

36. Hirokawa, N., T. C. Keller III, R. Chasan, and M. S. Mooseker. 1983. Mechanism of brush border contractility studied by quick-freeze, deep-etch method. *J. Cell Biol.* 96:1325–1336.

37. Hynes, R. O., A. T. Destree, and D. D. Wagner. 1982. Relationship between microfilaments, cell-substratum adhesion and fibronectin. *Cold Spring Harbor Symp. Quant. Biol.* 46:659–670.

38. Isenberg, G., P. C. Rathke, N. Hülsmann, W. W. Franke, and K. E. Wohlfahrth-Bottermann. 1976. Cytoplasmic actomyosin fibrils in tissue culture cells. Direct proof of contractility by visualization of ATP-induced contraction in fibrils isolated by laser microbeam dissection. *Cell Tissue Res.* 166:427–443.

39. Kreis, T. E., and W. Brichmeier. 1980. Stress fiber sarcomeres of fibroblasts are contractile. *Cell.* 22:555–561.

40. Langanger, G., J. De Mey, M. Moeremans, G. Daneels, M. De Brabander, and J. V. Small. 1984. Ultrastructural localization of α-actinin and filamin in cultured cells with the immunogold staining (IGS) method. *J. Cell Biol.* 99:1324–1334.

41. Lark, M. W., J. Laterra, and L. A. Culp. 1985. Close and focal adhesions of fibroblasts to a fibronectin containing matrix. *Fed. Proc.* 44:394–403.

42. Larsen, W. J., H.-N. Tung, S. A. Murray, and C. A. Swenson. 1979. Evidence for the participation of actin microfilaments and bristle coats in the internalization of gap junction membrane. *J. Cell Biol.* 83:576–587.

43. Lazarides, E., and K. Burridge. 1975. α-Actinin: immunofluorescent localization of a muscle structural protein in nonmuscle cells. *Cell.* 6:289–298.

44. Lübbers, D. W., G. Hauck, H. Weigelt, and K. Addicks. 1979. Contract-

ile properties of frog capillaries tested by electrical stimulation. *Bibl. Anat.* 17:3–10.

45. Mangeat, P., and K. Burridge. 1984. Actin-membrane interaction in fibroblasts: what proteins are involved in this association? *J. Cell Biol.* 99 (1, Pt. 2):95s–103s.

46. Maupin, P., and T. D. Pollard. 1983. Improved preservation and staining of HeLa actin filaments, clathrin-coated membrane, and other cytoplasmic structures by tannic acid-glutaraldehyde-saponin fixation. *J. Cell Biol.* 96:51–62.

47. Michel, G. C., and M. E. Phillips. 1984. Effects of Ca^{2+} ionophore, A 23187, on permeability of single vessels. *Int. J. Microcirc.* 3:361. (Abstr.).

48. Niederman, R., and T. D. Pollard. 1975. Human platelet myosin. II. In vitro assembly and structure of myosin filaments. *J. Cell Biol.* 67:72–92.

49. Pollard, T. D. 1975. Electronmicroscopy of synthetic myosin filaments. Evidence for cross-bridge flexibility and copolymer formation. *J. Cell Biol.* 67:93–104.

50. Pollard, T. D. 1981. Cytoplasmic contractile proteins. *J. Cell Biol.* 91 (3, Pt. 2):156s–165s.

51. Pollard, T. D. 1982. Myosin purification and characterization. *Methods Cell Biol.* 24:333–370.

52. Pollard, T. D., S. M. Thomas, and R. Niederman. 1974. Human platelet myosin. I. Purification by a rapid method applicable to other nonmuscle cells. *Anal. Biochem.* 60:258–266.

53. Ruoslahti, E., E. Engvall, and E. G. Hayman. 1974. Fibronectin: current concepts of its structure and function. *Collagen Relat. Res.* 1:95–128.

54. Ruoslahti, E., M. Vuento, and E. Engvall. 1978. Interaction of fibronectin with antibodies and collagen in radioimmunoassay. *Biochim. Biophys. Acta.* 534:210–218.

55. Sanger, J. H., and J. W. Sanger. 1980. Banding and polarity of actin filaments in interphase and cleaving cells. *J. Cell Biol.* 86:568–575.

56. Scholey, J. M., R. C. Smith, D. Drenckhahn, U. Gröschel-Stewart, and J. Kendrick-Jones. 1982. Isolation and characterization of myosin from calf thymus and thymic lymphocytes, and studies on the effect of phosphorylation of its M_r = 20,000 light chain. *J. Biol. Chem.* 257:7737–7745.

57. Singer, I. I. 1979. The fibronexus: a transmembrane association of fibronectin-containing fibres and bundles of 5 nm microfilaments in cultured human fibroblasts. *Cell.* 24:481–492.

58. Singer, I. I., and P. R. Paradiso. 1981. A transmembrane association of fibronectin-containing fibres and bundles of 5 nm microfilaments in hamster and human fibroblasts. *Cell.* 16:657–685.

59. Singer, I. I., D. W. Kawka, D. M. Kazazis, and R. A. F. Clark. 1984. In vivo co-distribution of fibronectin and actin fibers in granulation tissue: immunofluorescence and electron microscopic studies of the fibronexus at the myofibroblast surface. *J. Cell Biol.* 98:2091–2106.

60. Squire, J. M. 1981. The Structural Basis of Muscular Contraction. Plenum Press, New York. 698 pp.

61. Starger, J. H., W. E. Brown, A. E. Goldman, and R. D. Goldman. 1978. Biochemical and immunological analysis of rapidly purified 10 nm filaments from baby hamster kidney (BHK-21) cells. *J. Cell Biol.* 78:93–109.

62. Timpl, R., J. Engel, and G. R. Martin. 1983. Laminin - a multifunctional proteins of basement membranes. *Trends Biochem. Sci.* 8:207–209.

63. Weber, K., and U. Gröschel-Stewart. 1974. Antibody to myosin: the specific visualization of myosin-containing filaments in nonmuscle cells. *Proc. Natl. Acad. Sci. USA.* 71:4561–4564.

64. Weigelt, H. 1982. Die spezialisierte Endothelzelle-erregbare Zelle und mechanischer Effektor der Mikrozirkulation. *Funkt. Biol. Med.* 1:53–60.

65. White, G. E., M. A. Gimbrone, and K. J. Fujiwara. 1983. Factors influencing the expression of stress fibers in vascular endothelial cells in situ. *J. Cell Biol.* 97:416–425.

66. Willingham, M. C., K. M. Yamada, S. S. Yamada, J. Pouyssegur, and I. Pastan. 1977. Microfilament bundles and cell shape are related to adhesiveness to substratum and are dissociable from growth control in cultured fibroblasts. *Cell.* 10:375–380.

67. Wong, A. J., T. D. Pollard, and I. Herman. 1983. Actin filament stress fibers in vascular endothelial cells in vivo. *Science (Wash. DC).* 219:867–869.

68. Yerna, M.-J., M. Aksoy, D. J. Hartshorne, and R. D. Goldman. 1978. BHK-21 myosin: isolation, biochemical characterization and intracellular localization. *J. Cell Sci.* 31:411–425.